

Macromolecular Chemistry and Physics

Elimination of the crystallinity of long polyethylene oxide-based copolymers for gas separation membranes by using electron beam irradiation

--Manuscript Draft--

Manuscript Number:	macp.201600441R1
Full Title:	Elimination of the crystallinity of long polyethylene oxide-based copolymers for gas separation membranes by using electron beam irradiation
Article Type:	Full Paper
Section/Category:	
Keywords:	Polyethylene oxide - copolymers Electron beam irradiation - crosslinking Crystallinity Carbon dioxide (CO ₂) Gas separation membrane
Corresponding Author:	ALBERTO TENA, Dr. Universidad de Valladolid Valladolid, Castilla y León SPAIN
Corresponding Author Secondary Information:	
Corresponding Author's Institution:	Universidad de Valladolid
Corresponding Author's Secondary Institution:	
First Author:	Angel Marcos-Fernández
First Author Secondary Information:	
Order of Authors:	Angel Marcos-Fernández Esbaide Adem Alejandra Rubio Hernández-Sampelayo Jose E. Báez Laura Palacio Pedro Pradanos ALBERTO TENA, Dr. Antonio Hernández
Order of Authors Secondary Information:	
Abstract:	PEO-based polymers containing long PEO chains are one of the best materials for post-combustion processes, attending to their separation properties. Optimal conditions for the application of the membrane separation module would be immediately after elimination of water vapor, NO _x , SO ₂ and dust particles, where the temperature of the gas is between 25 and 40 °C., Materials with high contents and longer length of PEO would be the ideal candidate for the application in terms of properties. Unfortunately, these materials are normally not applicable due to, at these temperatures, the high crystallinity of PEO chains which leads to poor gas separation properties. Here, by electron beam irradiation, we have been able to eliminate or substantially reduce the crystallinity of poly(ether-imide)s with high content in PEO, which was confirmed by the positive effect in the separation properties. Optimal dosage to eliminate the crystallinity and to maximize permeability has been investigated as well.
Additional Information:	
Question	Response

Please submit a plain text version of your cover letter here.

Please note, if you are submitting a revision of your manuscript, there is an opportunity for you to provide your responses to the reviewers later; please do not add them to the cover letter.

September 14th, 2016

Dear Editor,

I'm pleased to submit an original research article entitled "Elimination of the crystallinity of long polyethylene oxide-based copolymers for gas separation membranes by using electron beam irradiation" by Angel Marcos-Fernández, Esbaide Adem, A. Rubio Hernández-Sampelayo, Jose E. Báez, Laura Palacio, Pedro Prádanos, Alberto Tena, and Antonio Hernández for consideration for publication in *Macromolecular Chemistry and Physics*.

PEO-based materials are considering the best materials for the application as a polymer membrane in post-combustion processes. Numerous research groups around the globe, having very high scientific community acceptance of their results, are working on it. Some of these research groups already assume that, in order to be applied, the future of this materials is only possible by the reduction or elimination of the high level of crystallinity normally presents on the materials (as for example recently Liu et. al. in *Progress in Polymer Science* 2013, 38, 1089).

In this manuscript, we propose and experimentally prove the method which allows reduction and elimination of the crystallinity in PEO-based copolymers by electron beam irradiation. A rigorous treatment and characterization of the samples have been done in this very multidisciplinary and international work. Finally, the analysis of the separation properties confirms the crystallinity reduction effect, where the treated materials showed better separation properties than the original polymers. All this factors would favour the applicability of the PEO-based materials in important processes as post-combustion.

We believe that this manuscript is appropriate for publication in *Macromolecular Chemistry and Physics* because it describes an innovative method for the elimination of the crystallinity in a really popular family of polymers that are applied in very diverse applications.

The manuscript is completely original, and no part of it has been published and is not under consideration for publication elsewhere.

This very international work was supported by several projects as DGAPA-PAPIIT-UNAM in México; or Ministry of Science and Innovation MAT2014-52644-R and Spanish Junta de Castilla y León VA-248U13, in Spain. We declare that we have no conflict of interest to disclose.

Thank you for your consideration!

Sincerely,

Dr. Alberto Tena
Institute of Polymer Research, Helmholtz-Zentrum Geesthacht
Max-Planck-Str. 1
21502 Geesthacht, Germany
Tel.: +49 4152 87 2448
Fax.: +49 4152 87 2466
E-mail: alberto.tena@hzg.de

Elimination of the crystallinity of long polyethylene oxide-based copolymers for gas separation membranes by using electron beam irradiation.

Angel Marcos-Fernández¹, Esbaide Adem², Alejandra Rubio Hernández-Sampelayo¹, Jose E. Báez³, Laura Palacio⁴, Pedro Prádanos⁴, Alberto Tena^{4*}^a, and Antonio Hernández⁴

¹*Instituto de Ciencia y Tecnología de Polímeros, CSIC, Juan de la Cierva 3, 28006 Madrid, Spain.*

²*Instituto de Física, Universidad Nacional Autónoma de México (UNAM), Circuito Exterior, Ciudad Universitaria, 04510, México D.F., México.*

³*Department of Chemistry, University of Guanajuato (UG), Noria Alta S/N, 36050, Guanajuato, Gto. México*

⁴*Smap UA-UVA_CSIC, Universidad de Valladolid, Facultad de Ciencias, Real de Burgos s/n, 47071 Valladolid, Spain.*

***Corresponding author email: alberto.tena@hzg.de**

^aPresent address: Helmholtz-Zentrum Geesthacht, Institute of Polymer Research, Max-Planck-Str. 1, 21502 Geesthacht, Germany.

Abstract

PEO-based polymers containing long PEO chains are one of the best materials for *post-combustion* processes, attending to their separation properties. Optimal conditions for the application of the membrane separation module would be immediately after elimination of water vapor, NO_x, SO₂ and dust particles, where the temperature of the gas is between 25 and 40 °C. Materials with high contents and longer length of PEO would be the ideal candidates for the application in terms of properties. Unfortunately, these materials are normally not applicable due to,

1 at these temperatures, the high crystallinity of PEO chains, which leads to poor gas separation
2 properties. Here, by electron beam irradiation, we have been able to eliminate or substantially
3 reduce the crystallinity of poly(ether-imide)s with high PEO content, which was confirmed by the
4 positive effect in the separation properties. Optimal dosage to eliminate the crystallinity and to
5 maximize permeability has been investigated.
6
7
8
9
10

11 **1. Introduction**

12
13 Gas separation membranes of polyethylene oxide (PEO) based materials are very interesting
14 for processes where the carbon dioxide is involved, such as pre- and post-combustion processes,
15 because of their excellent performance for CO₂ removal. PEO consists of polar ether groups, which
16 can produce quadrupole interactions with CO₂. It leads to the known high affinity of PEO towards
17 CO₂. Eventually, it contributes to a higher selectivity during the gas separation process^[1].
18
19
20
21
22
23
24
25
26
27
28

29 Long PEO chains can crystallize, and crystallinity has an enormous influence in the properties of
30 the materials including their gas separation properties since crystals are non-permeable entities^[1].
31 PEO crystals have a relatively low melting temperature, below 76 °C^[2]. Using PEO-containing
32 materials at temperatures above PEO melting point would be enough to have it in amorphous state.
33
34 In the case of gas separation membranes, the permeability of the PEO-based materials would
35 increase, but the selectivity is also affected by the temperature, and typically it would be strongly
36 reduced. As an example, commercial PEBA[®] or Polyactive[®] polymers have selectivities close to 60
37 at 20 °C for the CO₂/N₂ pair, while at 50 °C the selectivity is almost halved^[3, 4]. Therefore, lower
38 temperatures during the process will result in lower permeabilities but higher selectivities, which is
39 crucial to have a better separation factor and to reduce membrane area^[5]. In the post-combustion
40 process, in general, there is an initial step where the gas is cooled in order to remove most of the
41 water vapor, NO_x, SO₂ and dust particles^[5, 6]. After this step, the gas is ready to pass through the
42 membrane at temperatures between 25 and 40 °C and any subsequent heating step would be
43
44
45
46
47
48
49
50
51
52
53
54
55
56
57
58
59
60
61
62
63
64
65

1 energetically inefficient. Thus, as already mentioned by Liu et al.^[7], the reduction of the
2 crystallinity of the PEO-based polymers is a critical point for the development and applicability of
3 these polymers as gas separation membranes. In addition, PEO has a poor mechanical strength that
4 has to be improved in PEO based materials in order to find industrial applications.
5
6
7
8
9

10 Various strategies have been considered to overcome these drawbacks (high crystallization
11 tendency and a weak mechanical strength) in PEO: structural design of polymers via
12 copolymerization, physical blending with other polymers and crosslinking, among others. The
13 combination of PEO chains with poly(propylene oxide)^[8], poly(dimethyl siloxane)^[9] or other alkyl
14 groups^[10] have proved to reduce crystallinity and increase permeability in the polymers. When PEO
15 is copolymerized with other monomers that react to form rigid segments (aromatic polyimide
16 segments for example), a high selectivity is obtained almost regardless of the composition of the
17 rigid segments^[11-13]. With respect to the permeability, several parameters have been studied ^[7], and
18 it was found that the main parameters were the content and the chain length of the PEO segments
19 in the polymer^[14, 15]. In general, higher content generates a continuous PEO phase which favors the
20 permeability^[16], and higher chain length promotes richer polyether areas, which favors the diffusion
21 of the gas through the polymer^[12, 17].
22
23
24
25
26
27
28
29
30
31
32
33
34
35
36
37
38
39

40 Incorporation of short PEO chains as an additive by physical blending improves
41 permeability and reduces crystallinity of the samples^[18, 19], but because there is not a covalent bond
42 between the polymer matrix and the PEO short chains, a leaching of the later takes place and
43 separation properties are worsened with time^[20].
44
45
46
47
48
49
50

51 With crosslinking, the inter-polymer chain spacing is modified and therefore it can be used to
52 quantitatively affect the free volume in the resultant network. Most of the PEO crosslinked gas
53 separation membranes have been built from PEO oligomers with (meth)acrylate chain ends that
54 polymerize to form a network^[21-24]. For these systems, the chemical composition of the crosslinker
55
56
57
58
59
60
61
62
63
64
65

1 plays an important role in modifying the gas transport properties of the polymers. In general, these
2 highly-rubbery crosslinked structures presented high CO₂ permeability values and good values for
3 the separation CO₂/H₂ with special interest in the case of elevated feed pressures^[25, 26], but the
4 results for the separation CO₂/N₂ are not so high (high-selective materials are required for this
5 separation). Another approach was the crosslinking of polymers with PEO chains, as for example
6 the crosslinking of Matrimid with amine terminated PEO^[27]. For this system, PEO length was
7 critical, thus, a 2000 g·mol⁻¹ molecular weight gave good gas separation results whereas a 600
8 g·mol⁻¹ molecular weight was not suitable due to the poor mechanical strength of the membrane^[28].

19 So far, to our knowledge, ionizing radiation has not been considered as crosslinking agent
20 for PEO based gas separation membranes. Linear pure PEO has been already crosslinked by using
21 ionizing radiation (gamma rays, electron beam), mainly for the production of hydrogels for
22 biomedical applications^[29-32], but also for the preparation of a dry polymer electrolyte in a lithium
23 ion battery^[33].

33 Ionizing radiation is known to produce changes in polymers such as scission, crosslinking
34 and oxidation of polymer chains^[34]. A FDA study concluded that all types of ionizing radiation
35 (electron beam, gamma rays and X-ray) treatments were equivalents in terms of the type and levels
36 of radiolysis products generated during irradiation^[35]. It has been shown that when linear pure PEO
37 was crosslinked with ionizing radiation in water or methanol solutions, both crosslinking and chain
38 scission took place^[31, 36, 37]. Gel content was slightly dependent on the molecular weight of the
39 linear PEO with final gel content values in between 60 and 80%^[28,30]. The minimum dose for the
40 formation of a PEO gel in water solution, when irradiated with gamma rays, was found to increase
41 with the increase in PEO concentration and a final value of approximately 100 kGy was needed at
42 25 °C for 100% pure linear PEO of 14400 g·mol⁻¹ molecular weight. This value was slightly lower
43 when irradiation was carried out at 80 °C^[34].

1
2
3
4
5
6
7
8
9
10
11
12
13
14
15
16
17
18
19
20
21
22
23
24
25
26
27
28
29
30
31
32
33
34
35
36
37
38
39
40
41
42
43
44
45
46
47
48
49
50
51
52
53
54
55
56
57
58
59
60
61
62
63
64
65

In our previous work with PEO based copoly(ether-imide)s membranes, the best gas separation results were attained for copolymers with a good phase-separated morphology (achieved through thermal treatment) and long PEO chains^[38, 39]. However, long PEO chains crystallized substantially reducing permeability and permeation measurements had to be performed at temperatures above the melting point of PEO chains. An increment in temperature leads to an increase in the permeability but decrease in the selectivity^[12, 39].

In this work, electron beam irradiation was applied to copoly(ether-imide)s with long PEO chains (6000 g·mol⁻¹) to reduce and ultimately suppress PEO crystallinity in a simple way without affecting the chemical structure and the morphology of the copolymer. The effect of the absorbed dose in the thermal properties and its relationship with the gas separation properties were studied.

2. Experimental

2.1. Synthesis of copoly(ether-imide)s

The copoly(ether-imide)s used here were prepared from 3,3',4,4'-benzophenonetetracarboxylic dianhydride (BKDA), polyoxyethylene-bis(amine) with nominal molecular weight of 6000 g·mol⁻¹ (PEO6000) and 4,4'-oxydianiline (ODA). **The diamines** PEO6000 and ODA were reacted in weight ratios 2:1, 4:1 and 6:1 with BKDA giving a polyoxyethylene **weight** content in the final polymer of 44.2, 60.4 and 68.9% respectively. The resulting copoly(ether-imide)s (**see chemical structure in Table 1**) were designated PEO-44, PEO-60 and PEO-69 respectively **according to the weight content of polyethylene oxide in the copolymers**. The synthesis of the polymers and the film preparation are described in Marcos-Fernández *et al.*^[40]. Before irradiation, films were thermally treated at 220 °C for 30 minutes to improve phase separation of the polyether and the polyimide blocks.

2.2. Electron beam irradiation

1 Samples with different dimensions were treated by electron beam irradiation. They were
2 introduced into 9 cm x 6 cm polyethylene bags and placed in a holder for heating to 70 °C. The
3 device was specially designed and purpose built at the Institute of Physics, UNAM. The samples
4 were irradiated at 70 °C with an electron-beam accelerator, using a Van de Graaff source,
5 1.3MeV energy and a beam current of 5 μA at a dose rate of 23.6 kGy·min⁻¹. Doses covered the
6 range 50–16000 kGy in air.
7
8
9
10
11
12
13

14 **2.3. Characterization methods**

15
16
17 For calorimetric studies, disc samples of 6 mm diameter were cut from the films. Differential
18 scanning calorimetry (DSC) analyses were carried out in a Mettler Toledo (DSC 822e) calorimeter
19 equipped with a liquid nitrogen accessory. Disc samples weighing 5–15 mg were sealed in
20 aluminum pans. Samples were heated with the following method: from 25 °C to 80 °C at 10 °C·min⁻¹;
21 from 80 °C to -90 °C at the maximum cooling rate accessible for the instrument; isotherm at -90
22 °C for 10 min; from -90 °C to 80 °C at 10 °C·min⁻¹. All scans were carried out under a constant
23 nitrogen purge. The melting point (T_m) is given as the maximum of the endothermic transition.
24 Glass transition temperature (T_g) is given as the midpoint of the change in heat capacity. The
25 percent of crystallinity of the PEO (X_c) respect to the PEO content in the copolymer was calculated
26 from the endothermic peak area ΔH_c corrected to the amount of PEO in the copolymer using the
27 following equation: $X_c = (\Delta H_c / \Delta H_0) \cdot 100$, where ΔH_0 is the melting enthalpy of PEO taken from
28 literature as 8.67 kJ·mol⁻¹[41].
29
30
31
32
33
34
35
36
37
38
39
40
41
42
43
44
45
46

47 **2.4. Gas permeation and selectivity**

48 He, O₂, N₂, CH₄ and CO₂ permeabilities were measured by using a barometric constant
49 volume permeator and the *time-lag* operation method. Measurements were carried out at 30 °C and
50 50 °C and the applied pressure was 3 bar. A sketch of the device used has been shown elsewhere^[42].
51 Disc samples of 24 mm diameter cut from the films were used.
52
53
54
55
56
57
58
59
60
61
62
63
64
65

1 The strategy known as *time-lag* method, attributed to Daynes *et al.*^[43], is very appropriate to
2 determine permeability, diffusivity and solubility of a sample by a simple, rapid and accurate
3 method working under transitory regime. The method has been successfully applied to determine
4 polymer gas permeation by many authors^[44, 45]. Its theoretical framework along with its practical
5 possibilities and limits have been abundantly documented^[46].
6
7
8
9

10 The transient response downstream the membrane to a pressure step enables the time-lag, t_0 ,
11 to be easily computed. This parameter can be put, in terms of the diffusion coefficient, D , and the
12 thickness of the membrane Δx , as:
13
14
15
16
17
18
19
20

$$21 \quad t_0 = \frac{\Delta x^2}{6D} \quad (1)$$

22 The amount of gas transmitted at time t through the membrane is calculated from the
23 permeate pressure readings in the low-pressure side. The permeability coefficient can be obtained
24 directly from the flow rate into the downstream volume upon reaching the steady state. Solubility,
25 S , can be obtained from directly measured diffusivities and permeabilities as follows:
26
27
28
29
30
31
32
33
34
35

$$36 \quad S = \frac{P}{D} \quad (2)$$

37 The ideal selectivity can be defined as the ratio of pure gas permeabilities for each pair of gases.
38
39
40
41
42
43

44 **3. Results and discussion**

45 **3.1. Calorimetric studies**

46 Changes in thermal properties with dose (0, 50, 100, 150, 200, 300, 500, 1000, 2000, 4000, 6000,
47 8000, 10000, 12000, 16000 kGy) were measured by DSC. For some doses several samples were
48 tested to estimate the dispersion of the results. It has already been demonstrated that these
49 copoly(ether-imide)s present a phase separated structure with a PEO rich phase that can crystallize
50
51
52
53
54
55
56
57
58
59
60
61
62
63
64
65

1 partially and a totally amorphous polyimide rich phase with a T_g at high temperature^[40]. In the first
2 heating run, from ambient temperature to 80 °C, an endothermic peak related to the melting of PEO
3 crystals was found. After cooling, in the second heating run from -90 to 80 °C, a T_g was observed at
4 low temperatures (in some samples it could not be detected) for the amorphous PEO chains and an
5 endothermic peak related to the melting of PEO crystals at higher temperatures. **The values for PEO**
6 **T_m and X_c from the first heating run and T_g from the second heating run for the copoly(ether-**
7 **imide)s after irradiation at different doses are listed in Table 1.**

8
9
10
11
12
13
14
15
16
17
18 In Figure 1, the percentage of crystallized PEO (after irradiation at 70 °C with the PEO
19 segments melted) *versus* dose is represented. PEO segments can crystallize in a very low proportion
20 in the copolymer PEO-44 whereas PEO can crystallize extensively from the melt before irradiation
21 in the copolymers PEO-60 and PEO-69. Crystallization is slightly higher for the copolymer PEO-69
22 that has a higher amount of PEO in its structure. PEO crystallinity decreased almost linearly with
23 the increase in dose for all the copolymers until complete suppression of the crystallinity.
24
25
26
27
28
29
30
31
32

33 Ionizing radiation produces simultaneously chain scission and crosslinking on polymers, and
34 the relative weight of each mechanism depends on the polymer structure^[34]. If chain scission was
35 predominant, it would be expected that the shorter PEO chains produced would have more mobility
36 and could crystallize more easily, giving a higher amount of crystallized PEO. If crosslinking was
37 predominant, chain mobility would be reduced and crystallization would decrease, as found for
38 these copolymers.
39
40
41
42
43
44
45
46
47

48 The changes in the T_g value confirmed that crosslinking was the main mechanism present.
49 This result is in agreement with the results found for pure PEO for which gel contents of 60-80%
50 are obtained after irradiation in solution^[28,30]. As it can be seen in Figure 2, initially the T_g value
51 was practically constant for PEO-44 up to 2000 kGy, and for PEO-60 and PEO-69 decreased
52 slightly with dose until a value of approximately 4000 kGy. Above these doses, the PEO is
53
54
55
56
57
58
59
60
61
62
63
64
65

1 completely amorphous in the materials and T_g value increased almost linearly with the increase in
2 dose due to the movement restrictions imposed by the crosslinking.
3
4

5 In Figures 3 and 4, the maximum of the melting endotherm of PEO segments and the
6 calculated amount of crystallized PEO respectively **in the second heating run**, are shown. The
7 temperature of the maximum of the melting endotherm decreased monotonically with the increase
8 in the absorbed dose for all the copolymers. Similarly to the first heating run, the amount of
9 crystallized PEO decreased almost linearly with the increase in dose for all the copolymers until
10 complete suppression of the crystallinity at 4000 kGy for copolymer PEO-44, at 6000 kGy for
11 copolymer PEO-60 and at 8000 kGy (although it has almost disappeared at 6000 kGy) for
12 copolymer PEO-69.
13
14
15
16
17
18
19
20
21
22
23

24
25
26 **DSC results demonstrate that electron beam irradiation is effective on suppressing PEO**
27 **crystallinity on these copoly(ether-imide)s with complete suppression at a dose of 6000 kGy and**
28 **suppression of the crystallinity above ambient temperature at a dose of 4000 kGy.**
29
30
31
32

33 34 **3.2. Permeability test** 35

36
37 Permeation tests were carried out in order to analyze the effect of the elimination of
38 crystallinity by electron beam irradiation on the separation properties. **In general, higher amount of**
39 **PEO in the sample will increase the permeability of the samples^[47]. In this sense, non-irradiated**
40 copolymer PEO-44 does not to show good gas permeation properties ^[39], thus permeation studies
41 were not carried out on this material. Moreover PEO-69 was very fragile and the samples broke
42 when loaded in the permeation cell, thus gas permeation was only evaluated in PEO-60 copolymers.
43
44
45
46
47
48
49
50
51
52 The PEO crystallinity of the irradiated samples (X_c), calculated from the endotherm of the first DSC
53 heating run, see Figures 1 and 2, is presented in Table 1. The values of the glass transition
54 temperature, T_g , are also included.
55
56
57
58
59
60
61
62
63
64
65

1 The permeation experiments were carried out at two different temperatures: 30 °C when there
2 are some PEO crystals (for low absorbed doses) and 50 °C when all PEO is in an amorphous state.
3
4 He, O₂, CH₄,N₂ and CO₂ gases were tested. The CO₂/N₂ pair was analyzed in more detail due to it is
5
6 the main mixture of gases to be separated in post-combustions processes.
7
8
9

10 Figure 5 shows the CO₂ permeability at 30 °C as a function of the absorbed dose. CO₂
11 permeability increased until a maximum was reached and afterwards it decreased. The reduction on
12 PEO crystallinity (see Figure 1) produced an increase on permeability but when PEO crystallinity
13 was suppressed, and the increase in T_g (that is, the increase of the stiffness of PEO chains within the
14 amorphous PEO phase) due to crosslinking hindered permeation and reduced permeability at 6000
15 kGy to a value similar to the non-irradiated sample. It is remarkable the increase of around 37% in
16 the permeability in some cases. The elimination of the impermeable crystals from the copolymer
17 produced an increase in permeability for all the gases tested^[26].
18
19
20
21
22
23
24
25
26
27
28
29
30

31 The evolution of the carbon dioxide permeability at 50 °C as a function of the absorbed dose
32 was tested and it is showed in Figure 6. In this case the behavior is completely different. While at
33 30 °C, it was observed an initial increase in permeability for increasing dose, now there is a
34 continuous decrease of permeability when dose increases. Of course, for the permeability values at
35 30 °C, the initial increase of permeability was caused by the disappearance of the PEOcrystals. At
36 50 °C, the fundamental contribution that causes a decrease on the permeability is the increase on the
37 PEO chains crosslinking produced by the increase in dose. Obviously, the mobility of the PEO
38 chains is much lower, which reduces the diffusivity of the gas through the membrane.
39
40
41
42
43
44
45
46
47
48
49
50

51 The evolution of permeability versus the absorbed dose is similar for the other gases studied
52 as shown for measurements performed at 30 °C in Figure 7. Note that in all cases there are maxima
53 within the range of 2000 to 4000 kGy.
54
55
56
57
58
59
60
61
62
63
64
65

1 Referring to selectivities, Figure 8 shows that there is not significant influence of the dose on
2 the CO₂/N₂ selectivity. This is the case for the other pairs studied. These data confirm that the effect
3 of irradiation is to reduce the PEO crystallinity and does not affect the rest of the structure. This
4 behavior confirms the effectiveness of the irradiation treatment in the reduction of crystallinity; and
5 shows how it is possible to control the properties of the material by irradiation. This would make
6 possible using really large fragments of polyethylene oxide in copoly(ether-imide)s without the
7 undesirable effects of crystallinity that otherwise would decrease permeability.
8

9
10
11
12
13
14
15
16
17
18 As mentioned, mobility of the chain segments increases permeability because straighter paths
19 are accessible to each gas molecule. This reduces diffusive selectivity thus leaving as the main
20 contribution to selectivity the differences in solubility, which is also reduced because some decrease
21 in the internal surface should be expected. This leads to an experimentally confirmed decrease of
22 permeability with permeability building the so called permeability-selectivity trade-offs that turned
23 to be straights in a double log selectivity versus permeability plot (Robeson plots). In Figure 8 the
24 upper bonds for the selectivity versus permeability trade-off are shown as fitted by Robeson^[48] and
25 as predicted for different temperatures by Rowe *et al.*^[49]. Note that for permeation at 30 °C and
26 medium values of absorbed doses there is a nice increase in permeability without a significant loss
27 in selectivity.
28
29
30
31
32
33
34
35
36
37
38
39
40
41

42 **4. Conclusions**

43
44
45
46
47 Irradiation with electrons of films made of copoly(ether-imide)s based on a long chain PEO of
48 6000 g·mol⁻¹ produced an almost linear decrease in the PEO crystallinity until complete
49 suppression, and an almost linear increase in the T_g value once PEO is completely amorphous, with
50 the increase in dose. This behavior is consistent with crosslinking being the predominant
51 mechanism over chain scission. Suppression of PEO crystallinity led to an increase in permeability
52
53
54
55
56
57
58
59
60
61
62
63
64
65

1
2 and, once PEO crystallinity disappeared, crosslinking of the amorphous PEO chains decreased
3 permeability. Selectivity remained virtually constant with absorbed dose.
4
5
6
7

8
9 Acknowledgements: We acknowledge the financial support of DGAPA-PAPIIT-UNAM grant
10 IN-103516 in México and Ministry of Science and Innovation grant MAT2014-52644-R in Spain.
11
12 The Spanish Junta de Castilla y León contributed as well to the funding of this work through its
13 grant VA-248U13. We acknowledge the technical support provided by M. Vásquez and J. Galindo
14
15 from IF-UNAM in the irradiation of the samples.
16
17
18
19
20

21 Keywords: Polyethylene oxide, Electron beam irradiation, Crystallinity, Carbon dioxide
22
23 (CO₂), Gas separation membrane
24
25
26
27
28
29

30 References

- 31
32
33
34 [1] H. Lin, B. D. Freeman, *Journal of Membrane Science* **2004**, 239, 105.
35 [2] D. W. Van Krevelen, "Chapter 6 - Transition temperatures", in *Properties of Polymers (Third, completely*
36 *revised edition)*, Elsevier, Amsterdam, 1997, p. 129.
37 [3] J. Liljepärg, P. Georgopoulos, T. Emmler, S. Shishatskiy, *RSC Advances* **2016**, 6, 11763.
38 [4] A. Tena, S. Shishatskiy, V. Filiz, *RSC Advances* **2015**, 5, 22310.
39 [5] S. Zhao, P. H. Feron, L. Deng, E. Favre, E. Chabanon, S. Yan, J. Hou, V. Chen, H. Qi, *Journal of Membrane*
40 *Science* **2016**, 511, 180.
41 [6] M. Wang, A. Lawal, P. Stephenson, J. Sidders, C. Ramshaw, *Chemical Engineering Research and Design*
42 **2011**, 89, 1609.
43 [7] S. L. Liu, L. Shao, M. L. Chua, C. H. Lau, H. Wang, S. Quan, *Progress in Polymer Science* **2013**, 38, 1089.
44 [8] S. R. Reijerkerk, A. C. IJzer, K. Nijmeijer, A. Arun, R. J. Gaymans, M. Wessling, *ACS applied materials &*
45 *interfaces* **2010**, 2, 551.
46 [9] S. R. Reijerkerk, M. H. Knoef, K. Nijmeijer, M. Wessling, *Journal of membrane science* **2010**, 352, 126.
47 [10] W. Yave, A. Car, S. S. Funari, S. P. Nunes, K.-V. Peinemann, *Macromolecules* **2009**, 43, 326.
48 [11] A. Tena, Á. Marcos-Fernández, M. de la Viuda, L. Palacio, P. Prádanos, Á. E. Lozano, J. de Abajo, A.
49 Hernández, *European Polymer Journal* **2015**, 62, 130.
50 [12] A. Tena, A. Marcos-Fernandez, A. Lozano, J. de Abajo, L. Palacio, P. Prádanos, A. Hernández, *Chemical*
51 *Engineering Science* **2013**, 104, 574.
52 [13] A. Tena, A. Marcos-Fernández, A. E. Lozano, J. G. de la Campa, J. de Abajo, L. Palacio, P. Prádanos, A.
53 Hernández, *Journal of Membrane Science* **2012**, 387–388, 54.
54 [14] K.-i. Okamoto, M. Fujii, S. Okamoto, H. Suzuki, K. Tanaka, H. Kita, *Macromolecules* **1995**, 28, 6950.
55 [15] A. Tena, A. Marcos-Fernández, L. Palacio, P. Prádanos, A. E. Lozano, J. de Abajo, A. Hernández, *Journal*
56 *of Membrane Science* **2013**, 434, 26.
57
58
59
60
61
62
63
64
65

- 1 [16] A. Tena, M. de la Viuda, L. Palacio, P. Prádanos, Á. Marcos-Fernández, Á. E. Lozano, A. Hernández,
2 *Journal of Membrane Science* **2014**, 453, 27.
- 3 [17] A. Tena, A. Marcos-Fernández, A. E. Lozano, J. G. de la Campa, J. de Abajo, L. Palacio, P. Prádanos, A.
4 Hernández, *Industrial & Engineering Chemistry Research* **2013**, 52, 4312.
- 5 [18] A. Car, C. Stropnik, W. Yave, K.-V. Peinemann, *Separation and Purification Technology* **2008**, 62, 110.
- 6 [19] W. Yave, A. Car, K.-V. Peinemann, M. Q. Shaikh, K. Rätzke, F. Faupel, *Journal of Membrane Science*
7 **2009**, 339, 177.
- 8 [20] J. Lillepång, P. Georgopoulos, S. Shishatskiy, *Journal of Membrane Science* **2014**, 467, 269.
- 9 [21] Y. Hirayama, Y. Kase, N. Tanihara, Y. Sumiyama, Y. Kusuki, K. Haraya, *Journal of Membrane Science*
10 **1999**, 160, 87.
- 11 [22] V. A. Kusuma, S. Matteucci, B. D. Freeman, M. K. Danquah, D. S. Kalika, *Journal of Membrane Science*
12 **2009**, 341, 84.
- 13 [23] H. Lin, T. Kai, B. D. Freeman, S. Kalakkunnath, D. S. Kalika, *Macromolecules* **2005**, 38, 8381.
- 14 [24] H. Lin, E. Van Wagner, J. S. Swinnea, B. D. Freeman, S. J. Pas, A. J. Hill, S. Kalakkunnath, D. S. Kalika,
15 *Journal of Membrane Science* **2006**, 276, 145.
- 16 [25] S. Quan, S. Li, Z. Wang, X. Yan, Z. Guo, L. Shao, *Journal of Materials Chemistry A* **2015**, 3, 13758.
- 17 [26] L. Shao, S. Quan, X.-Q. Cheng, X.-J. Chang, H.-G. Sun, R.-G. Wang, *International Journal of Hydrogen*
18 *Energy* **2013**, 38, 5122.
- 19 [27] H.-Y. Zhao, Y.-M. Cao, X.-L. Ding, M.-Q. Zhou, J.-H. Liu, Q. Yuan, *Journal of Membrane Science* **2008**,
20 320, 179.
- 21 [28] H.-Y. Zhao, Y.-M. Cao, X.-L. Ding, M.-Q. Zhou, Q. Yuan, *Journal of Membrane Science* **2008**, 323, 176.
- 22 [29] C. Branca, S. Magazu, G. Maisano, L. Auditore, R. Barna, D. De Pasquale, U. Emanuele, A. Trifiro, M.
23 Trimarchi, *Journal of applied polymer science* **2006**, 102, 820.
- 24 [30] S. Kim, J. H. Kim, J. O. Kim, S. Ku, H. Cho, P. Huh, *Macromolecular Research* **2014**, 22, 131.
- 25 [31] E. W. Merrill, K. A. Dennison, C. Sung, *Biomaterials* **1993**, 14, 1117.
- 26 [32] F. Yoshii, Y. Zhanshan, K. Isobe, K. Shinozaki, K. Makuuchi, *Radiation Physics and Chemistry* **1999**, 55,
27 133.
- 28 [33] R. Uchiyama, K. Kusagawa, K. Hanai, N. Imanishi, A. Hirano, Y. Takeda, *Solid State Ionics* **2009**, 180, 205.
- 29 [34] A. Chapiro, *Nuclear Instruments and Methods in Physics Research Section B: Beam Interactions with*
30 *Materials and Atoms* **1995**, 105, 5.
- 31 [35] V. Komolprasert, "Packaging for foods treated with ionizing radiation", in *Packaging for nonthermal*
32 *processing of food*, J.H. Han, Ed., Blackwell Publishing 2007, p. 213.
- 33 [36] U. Gröllmann, W. Schnabel, *Die Makromolekulare Chemie* **1980**, 181, 1215.
- 34 [37] V. W. Schnabel, U. Borgwardt, *Die Makromolekulare Chemie* **1969**, 123, 73.
- 35 [38] D. M. Munoz, E. M. Maya, J. de Abajo, G. Jose, A. E. Lozano, *Journal of Membrane Science* **2008**, 323,
36 53.
- 37 [39] A. Tena, A. E. Lozano, L. Palacio, A. Marcos-Fernández, P. Prádanos, J. de Abajo, A. Hernández,
38 *International Journal of Greenhouse Gas Control* **2013**, 12, 146.
- 39 [40] A. Marcos-Fernández, A. Tena, A. E. Lozano, J. G. de la Campa, J. de Abajo, L. Palacio, P. Prádanos, A.
40 Hernández, *European Polymer Journal* **2010**, 46, 2352.
- 41 [41] D. W. Van Krevelen, "Chapter 5 - Calorimetric properties", in *Properties of Polymers (Third, completely*
42 *revised edition)*, Elsevier, Amsterdam, 1997, p. 109.
- 43 [42] J. Marchese, M. Anson, N. A. Ochoa, P. Prádanos, L. Palacio, A. Hernández, *Chemical Engineering*
44 *Science* **2006**, 61, 5448.
- 45 [43] H. A. Daynes, "The process of diffusion through a rubber membrane", *Proceedings of the Royal Society*
46 London, 1920.
- 47 [44] J. Crank, "The Mathematics of Diffusion", s.e.C. Press, Ed., Clarendon Press, Oxford, 1975.
- 48 [45] D. D. Paul, A.T., *Journal of polymer science* **1965**, 10, 17.
- 49 [46] S. W. Rutherford, D. D. Do, *Adsorption* **1997**, 3, 283.
- 50 [47] S. Quan, Y. P. Tang, Z. X. Wang, Z. X. Jiang, R. G. Wang, Y. Y. Liu, L. Shao, *Macromolecular Rapid*
51 *Communications* **2015**, 36, 490.
- 52 [48] L. M. Robeson, *Journal of Membrane Science* **2008**, 320, 390.
- 53
54
55
56
57
58
59
60
61
62
63
64
65

Figure Caption

Figure 1. Percentage of crystallized PEO vs dose for the first heating run from ambient temperature for the copoly(ether-imide)s.

Figure 2. T_g vs dose for the copoly(ether-imide)s.

Figure 3. Maximum of the melting endotherm in the second heating run vs dose for the copoly(ether-imide)s.

Figure 4. Percentage of crystallized PEO vs dose for the second heating run for the copoly(ether-imide)s.

Figure 5. CO₂ permeability of the PEO-60 irradiated membranes as a function of absorbed dose measured at 30 °C..

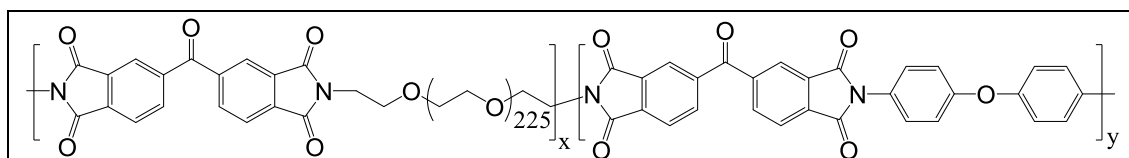
Figure 6. CO₂ permeability of the PEO-60 irradiated membranes as a function of absorbed dose measured at 50 °C.

Figure 7. Permeabilities for other gases as a function of the absorbed dose for PEO-60.

Figure 8. Robeson plot for the CO₂/N₂ pair measured at 30 °C (circles) and 50 °C (squares).

Tables

Table 1. Percentage of crystallinity (Xc) from the first heating run and PEO glass transition temperature (Tg) from the second heating run for the copoly(ether-imide)s after irradiation at different doses.



Sample	Dose (kGy)	PEO Xc / % 1st heating	PEO Tg / °C 2nd heating
PEO-44	0	1.2	-60.6
	1000	0.2	-62.2
	2000	0	-61.5
	4000	0	-46.8
	6000	0	-36.6
PEO-60	0	37.1	-
	1000	22.0	-47.7
	2000	1.7	-56.0
	4000	0.9	-55.3
	6000	0	-49.0
PEO-49	0	433	-43.2
	1000	30.6	-45.7
	2000	8.5	-46.6
	4000	0.4	-52.7
	6000	0	-54.3

Figures

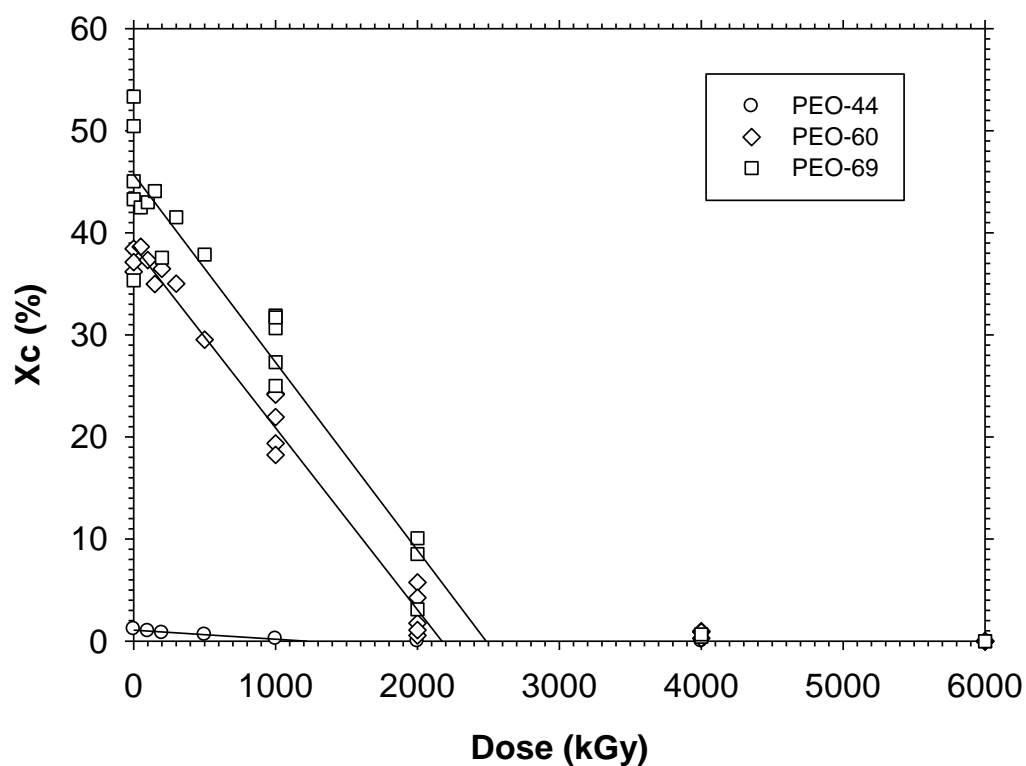


Figure 1. Percentage of crystallized PEO vs dose for the first heating run from ambient temperature for the copoly(ether-imide)s.

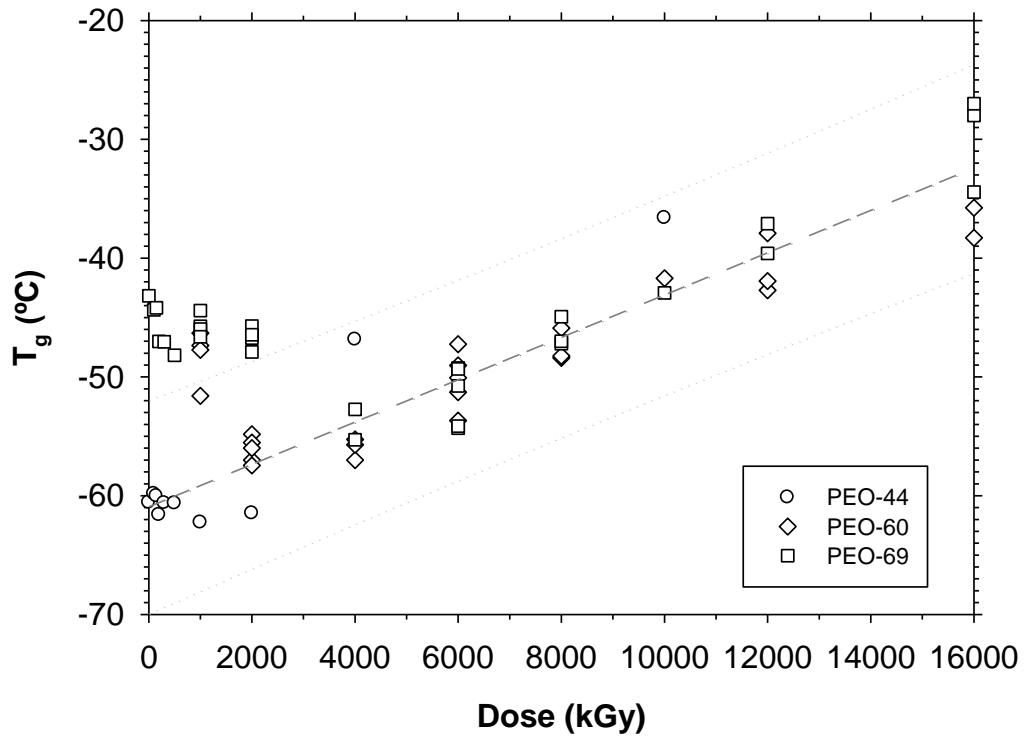


Figure 2. T_g vs dose for the copoly(ether-imide)s.

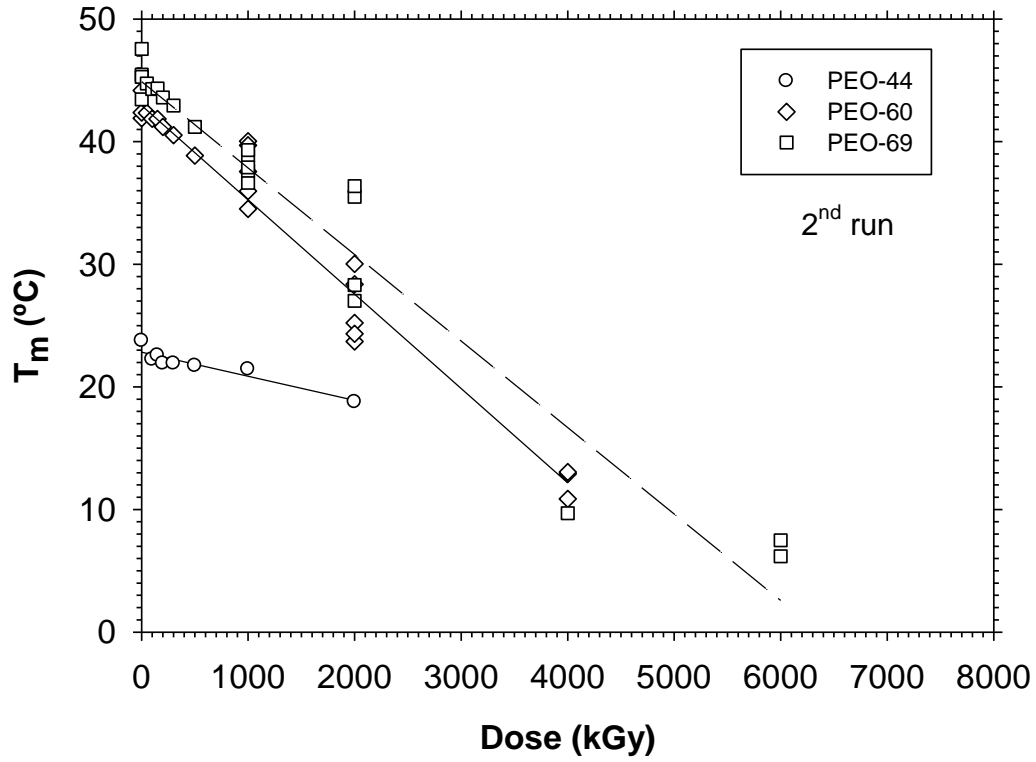


Figure 3. Maximum of the melting endotherm in the second heating run vs dose for the copoly(ether-imide)s.

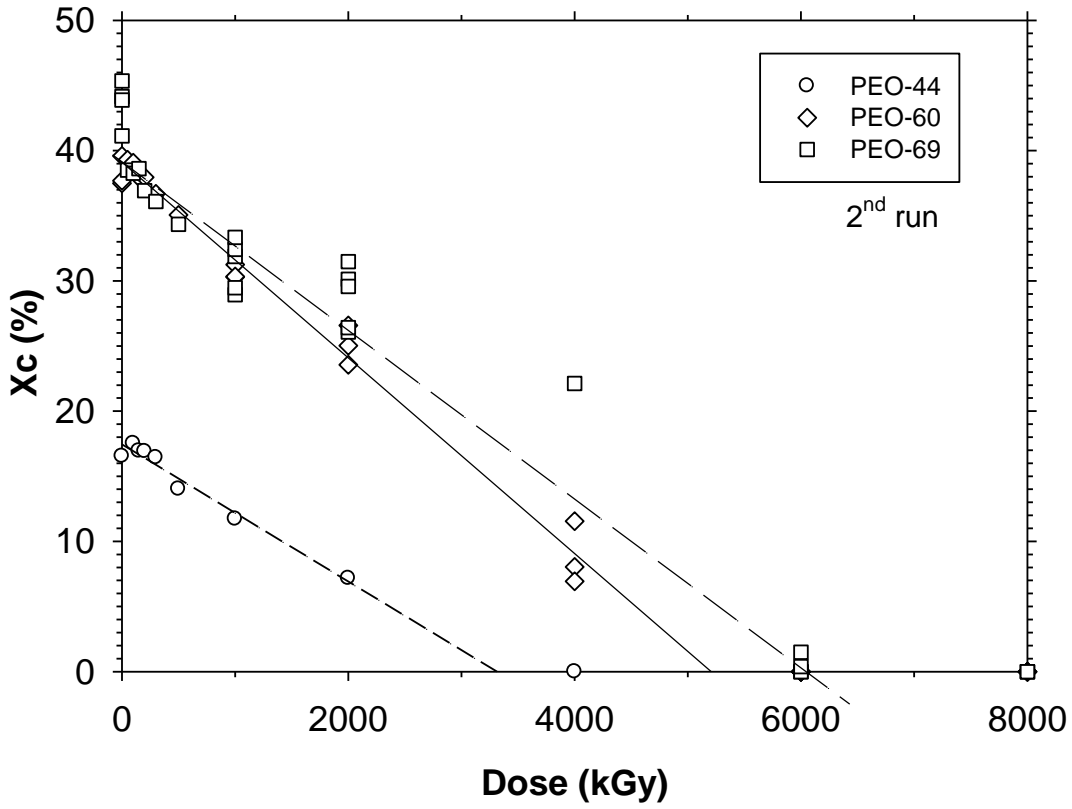


Figure 4. Percentage of crystallized PEO vs dose for the second heating run for the copoly(ether-imide)s.

1
2
3
4
5
6
7
8
9
10
11
12
13
14
15
16
17
18
19
20
21
22
23
24
25
26
27
28
29
30
31
32
33
34
35
36
37
38
39
40
41
42
43
44
45
46
47
48
49
50
51
52
53
54
55
56
57
58
59
60
61
62
63
64
65

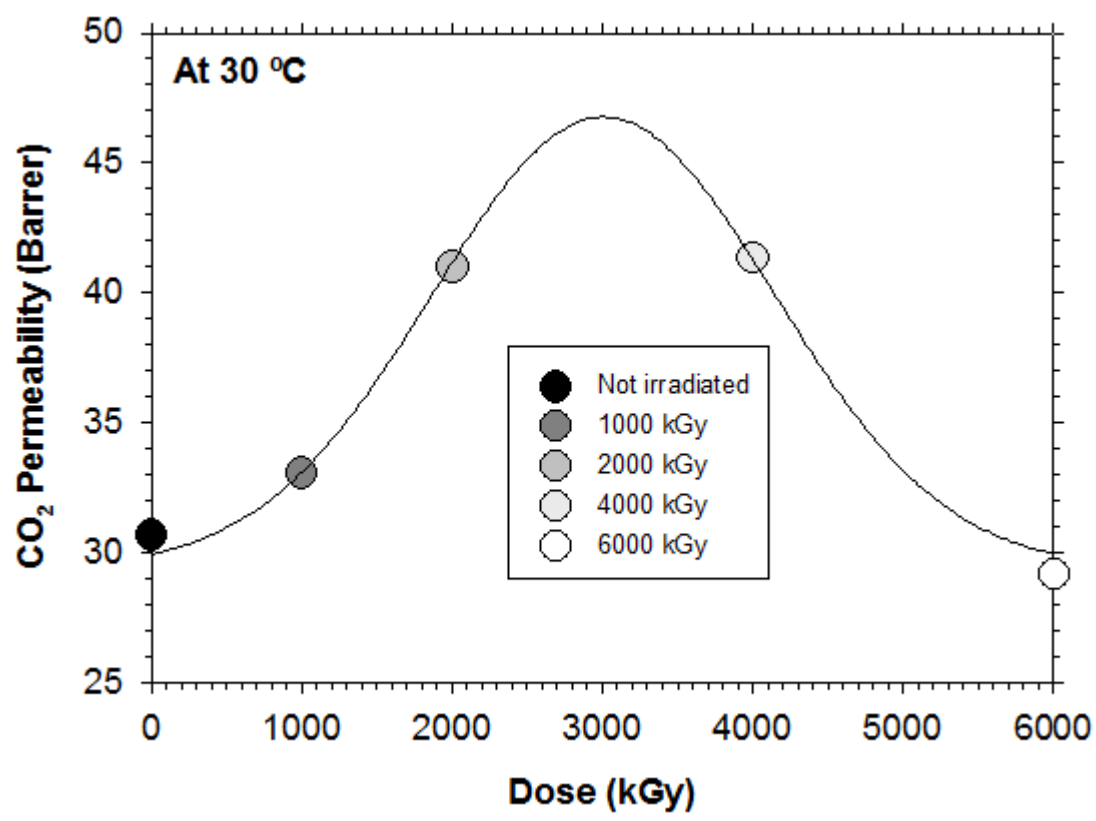


Figure 5. CO₂ permeability of the PEO-60 irradiated membranes as a function of absorbed dose measured at 30 °C.

1
2
3
4
5
6
7
8
9
10
11
12
13
14
15
16
17
18
19
20
21
22
23
24
25
26
27
28
29
30
31
32
33
34
35
36
37
38
39
40
41
42
43
44
45
46
47
48
49
50
51
52
53
54
55
56
57
58
59
60
61
62
63
64
65

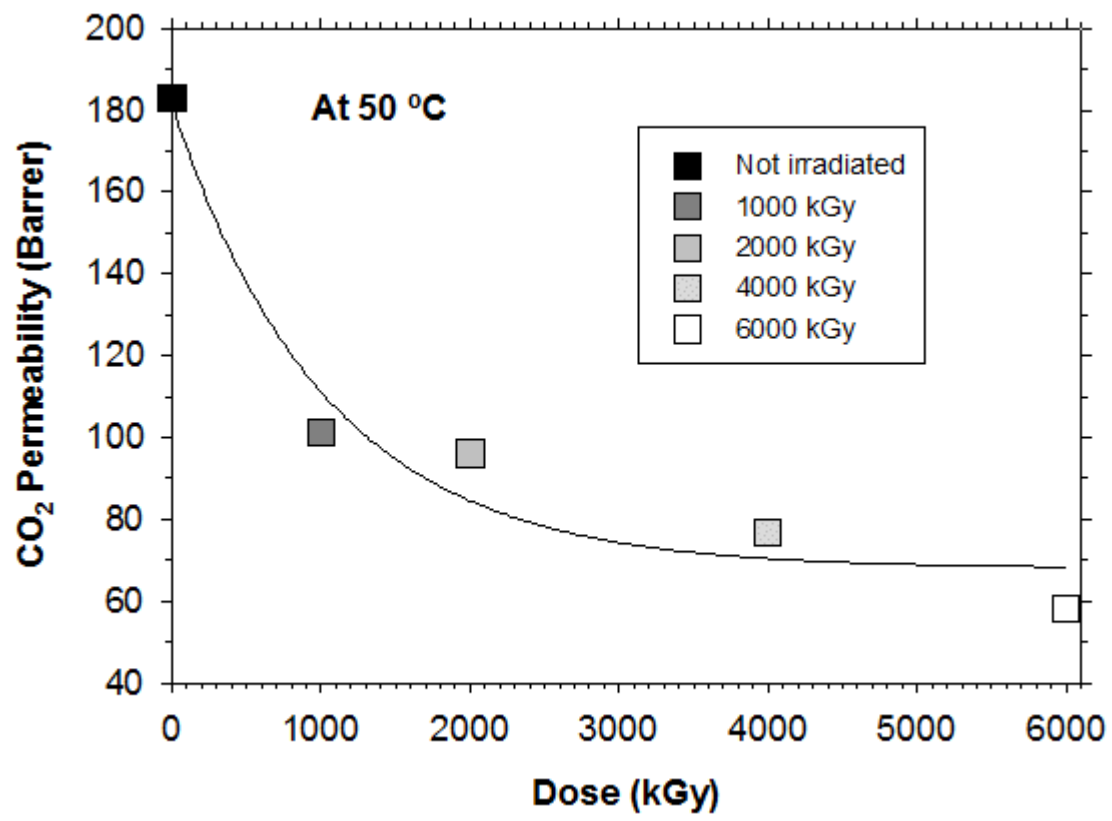


Figure 6. CO₂ permeability of the PEO-60 irradiated membranes as a function of absorbed dose measured at 50 °C.

1
2
3
4
5
6
7
8
9
10
11
12
13
14
15
16
17
18
19
20
21
22
23
24
25
26
27
28
29
30
31
32
33
34
35
36
37
38
39
40
41
42
43
44
45
46
47
48
49
50
51
52
53
54
55
56
57
58
59
60
61
62
63
64
65

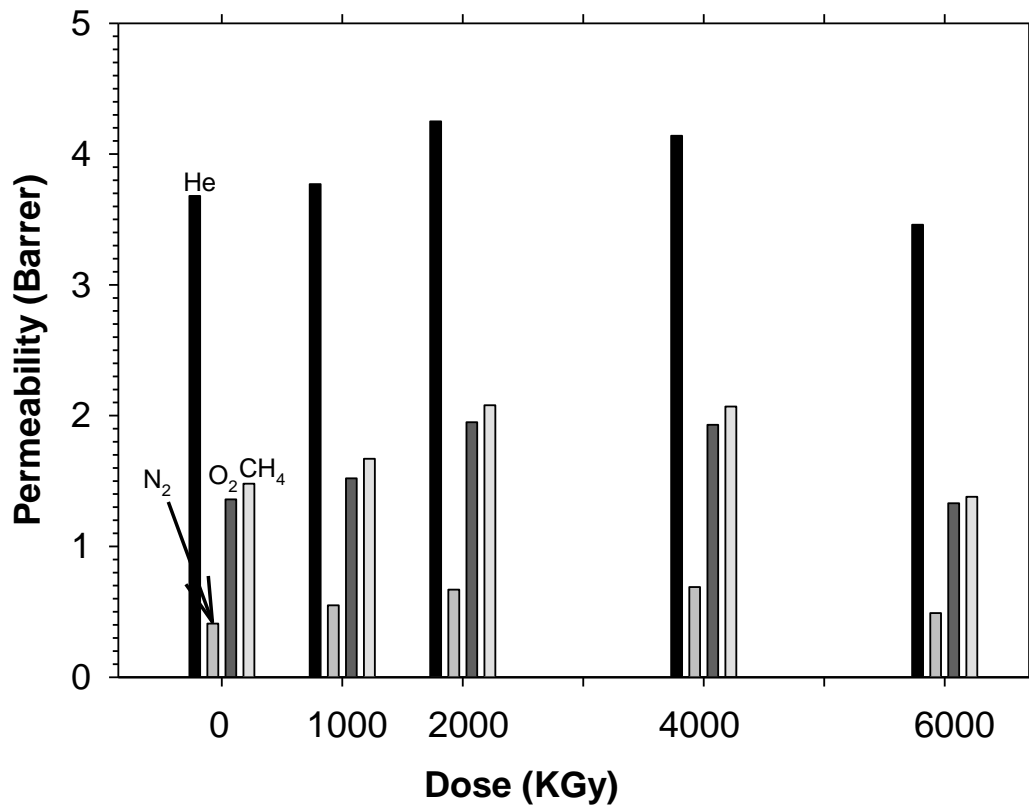


Figure 7. Permeabilities for other gases as a function of the absorbed dose for PEO-60.

1
2
3
4
5
6
7
8
9
10
11
12
13
14
15
16
17
18
19
20
21
22
23
24
25
26
27
28
29
30
31
32
33
34
35
36
37
38
39
40
41
42
43
44
45
46
47
48
49
50
51
52
53
54
55
56
57
58
59
60
61
62
63
64
65

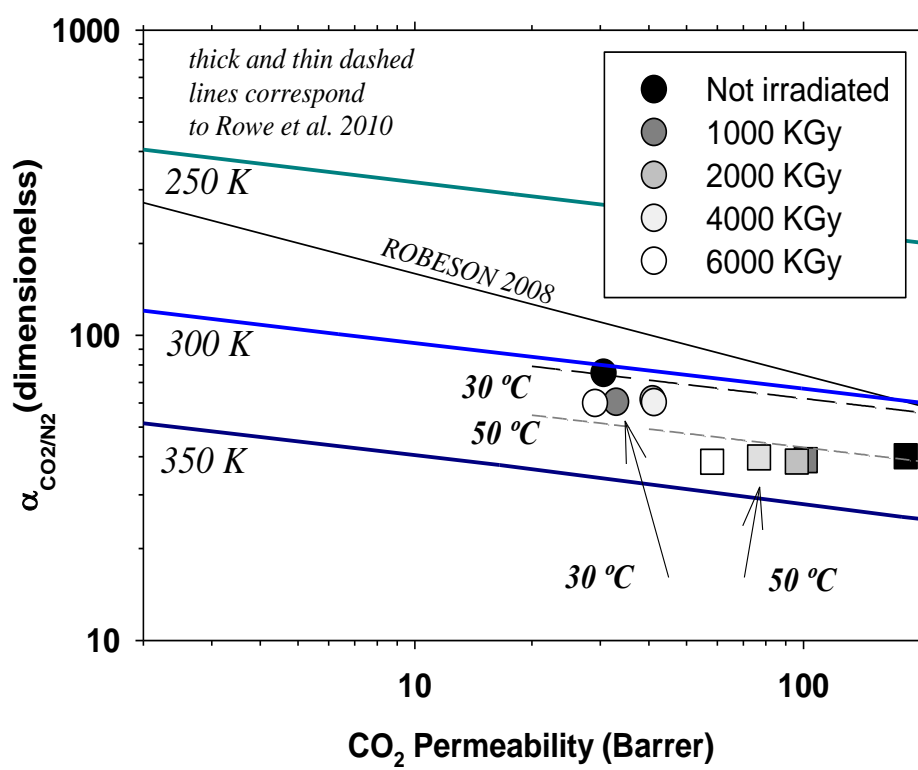
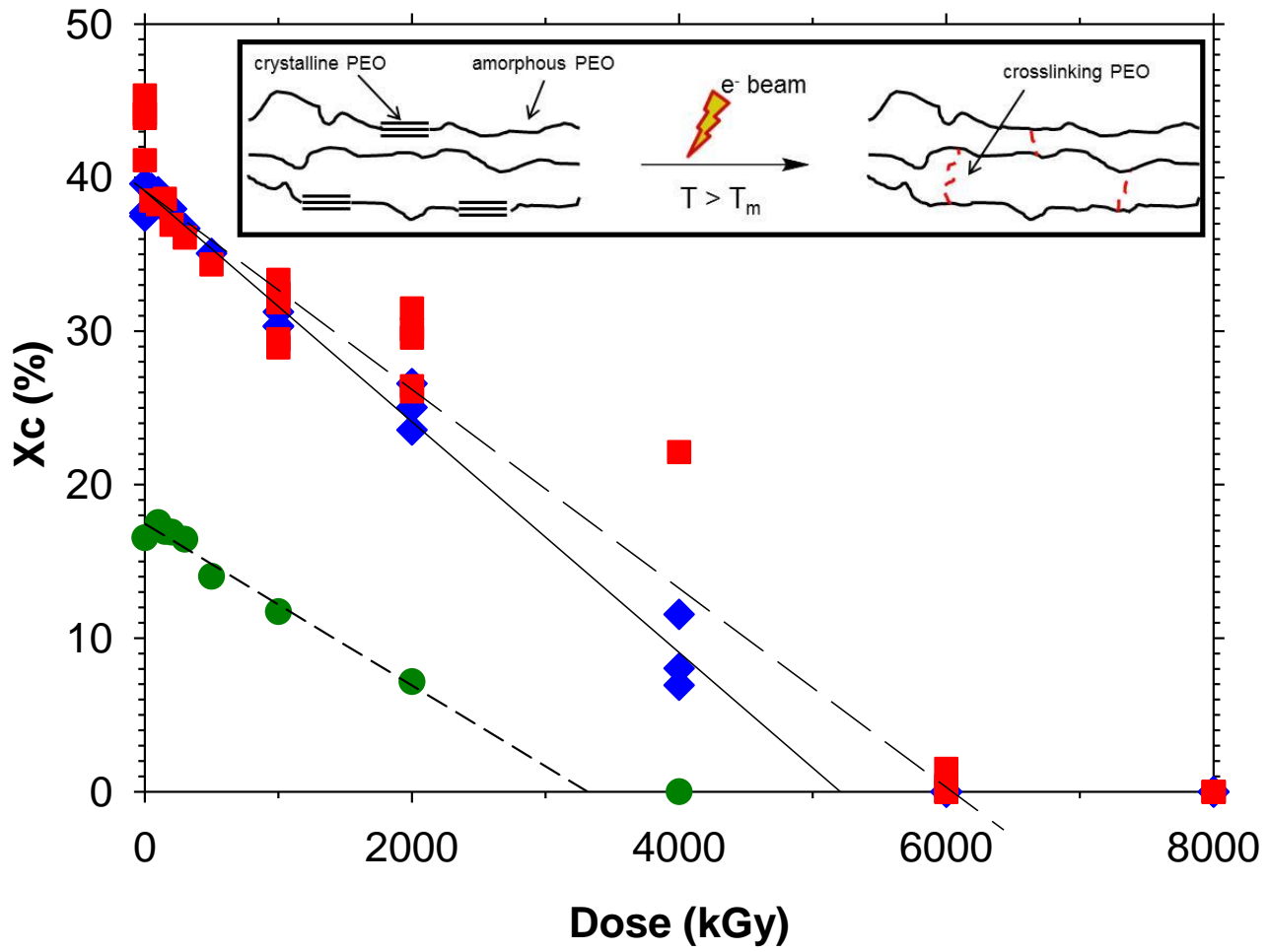


Figure 8. Robeson plot for the CO₂/N₂ pair measured at 30 °C (circles) and 50 °C (squares).

1
2
3
4
5
6
7
8
9
10
11
12
13
14
15
16
17
18
19
20
21
22
23
24
25
26
27
28
29
30
31
32
33
34
35
36
37
38
39
40
41
42
43
44
45
46
47
48
49
50
51
52
53
54
55
56
57
58
59
60
61
62
63
64
65

FIGURE FOR ToC_ABSTRACT





Click here to access/download
Production Data
production data.xlsx

